

1 **Appendix A: Application of frozen ground conditions and other EcH2O-iso adaptations**

2 Using Eqns 1-3 and 5, soil frost was estimated with a step-wise process using each soil layer (Carey and Woo, 2005). At the
3 beginning of each time-step, k_{fi} was estimated for each soil layer. With the thermal conductivity and the depth of frost in each
4 layer (z_{fi} , and conversely unfrozen depth, Δx), the thermal resistance of each layer was estimated ($R = z_{fi}/k_{fi}$). The depth of
5 frost in each layer has a maximum of the total depth of the layer. If the total resistance to freeze soil layer m is exceeded (i.e. $T_s >$
6 $N(m) = \lambda\theta\Delta x(\sum_{j=1}^{m-1} R(j))$, Carey and Woo, 2005), the soil layer is completely frozen. If the total resistance is not exceeded
7 then partial freezing/thawing of the soil layer occurs:

$$\Delta z_f = -k_f(m) \sum_{j=1}^{m-1} R(j) + \sqrt{k_f(m)^2 \left(\sum_{j=1}^{m-1} R(j) \right)^2 + \frac{2k_f(m)N}{\lambda\theta}} \quad \text{A.1}$$

8 where the sum of the terms $R(j)$ are the resistance of frozen soil layers up to the soil layer currently undergoing freezing, and Δz_f
9 is the increase/decrease in the depth of frost. The process is repeated each day to estimate the increase (freezing) or decreasing
10 (thawing) of the frost front.

11 The limitation of a single, non-depth dependent porosity and hydraulic conductivity in the model structure was modified as
12 a minor model structure change by using a simple exponential function to decrease the soil porosity and hydraulic conductivity
13 with depth, similar to the approach employed by Kuppel et al. (2018) for the rooting profile. Similar to the original model
14 structure, the approach assumes that the soil properties are the same for all soil layers (3), while increased consolidation of soils
15 at deeper depths result in lower porosity and lower hydraulic conductivity. The porosity is estimated for layer 1 as:

$$\phi_1 = k \cdot \phi \cdot \left(1 - \exp\left(-\frac{d_1}{k}\right) \right) / d_1 \quad \text{A.2}$$

16 where d_1 is the soil depth of layer 1, ϕ_o is the porosity at the soil surface, and k is the exponential rate of change of the porosity.
17 For layer 2:

$$\phi_2 = k \cdot \phi \cdot \left(\exp\left(-\frac{d_1}{k}\right) - \exp\left(-\frac{(d_1 + d_2)}{k}\right) \right) / d_2 \quad \text{A.3}$$

18 where d_2 is the depth of layer 2, and for layer 3:

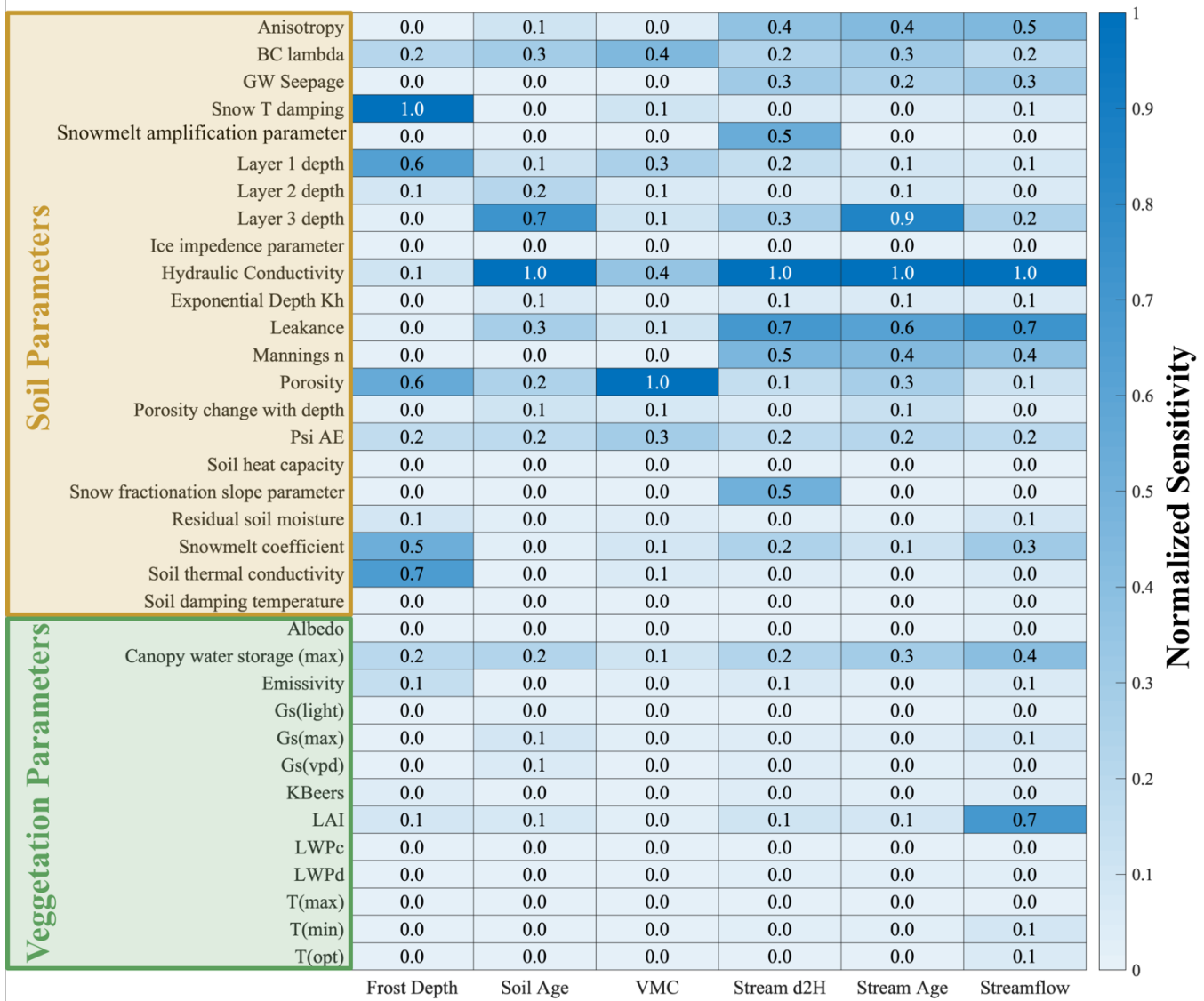
$$\phi_3 = k \cdot \phi \cdot \left(\exp\left(-\frac{d_1 + d_2}{k}\right) - \exp\left(-\frac{d}{k}\right) \right) / (d_1 + d_2) \quad \text{A.4}$$

19 where d is the total depth of the soil, the sum of all soil layer depths. Equations A.2-A.4 can also be used to solve for the
20 hydraulic conductivity in each soil layer (replace ϕ with K_h in each equation). The parameterization of k for both the porosity and
21 hydraulic conductivity with depth should be carefully chosen. Parameterization should always be checked to ensure that the
22 porosity in layer 3 is greater than the residual soil moisture (θ_r) and the permanent wilting point (θ_w).
23

24 **Appendix B: Morris sensitivity analysis**

25 The aid with parameterization and reduce the total number of parameters used within calibration of the EcH2O-iso model, a
26 sensitivity analysis with the Morris Sensitivity method and mean absolute error was used to assess how sensitive the model
27 parameters were to stream discharge, stream isotopes ($\delta^2\text{H}$), and soil moisture (calibration time-series). Since the vegetation
28 dynamics (carbon allocation mechanisms and vegetation growth) were not activated for the calibration, most vegetation
29 parameters were not included in the sensitivity analysis as they would not result in any changes to observable metrics. These

30 parameters include: leaf allocation parameters, canopy quantum efficiency parameters, cold stress, and moisture stress leaf
 31 turnover parameters. Parameter sensitivity was assessed using the radial step method and 50 different trajectories. Initial
 32 parameterizations were established using Latin Hypercube Sampling (LHS) to maximize the distance between the randomized
 33 trajectories. Each radial step deviated from the initial parameterization by progressively changing each parameter by half of the
 34 parameters range. For example, initial parameter value of 0.1 with a range of 2 (0 – 2) results in a new parameter value of 1.1
 35 (0.1 + (2-0)/2). The sensitivity of the parameter was assessed against the original parameterization for the trajectory using the
 36 mean absolute error.



37
 38 **Figure B.1.: Normalized mean absolute error for each time-series. Values of 1 indicate the most sensitive parameters and 0 indicates**
 39 **the least sensitive parameters. Additional information on the naming convention is found at [iso.readthedocs.io/en/latest/Setup.html](https://ech2o-

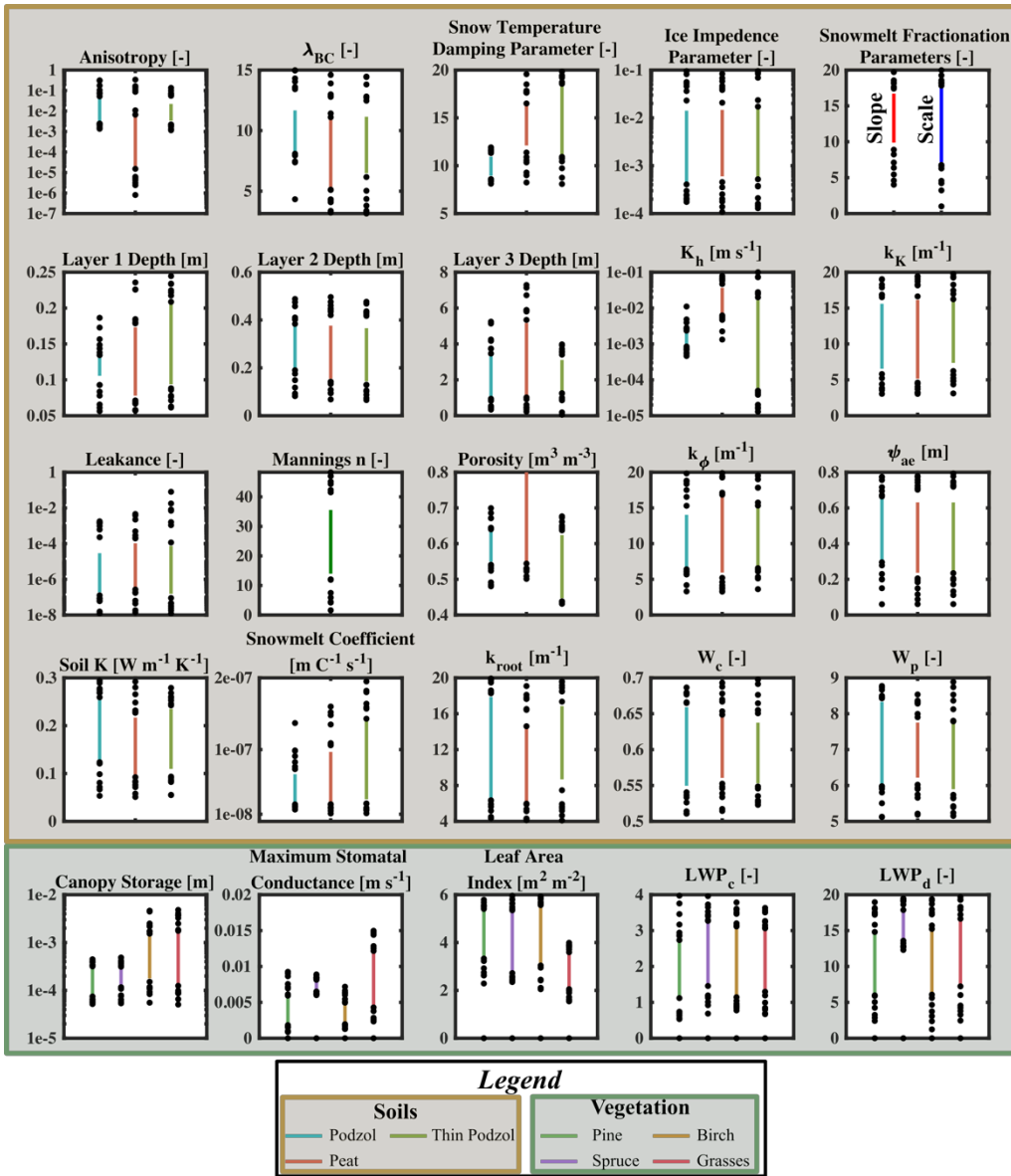
 40 <a href=)**

41 Mean absolute error was averaged for all trajectories to determine the mean sensitivity of each parameter. For streamflow, the
 42 parameters most sensitive are a mixture of soil parameters (e.g. hydraulic conductivity, snowmelt coefficient, and anisotropy),
 43 channel parameters (e.g. Mannings n and leakance), and vegetation parameters (e.g. leaf area index and canopy water storage).
 44 Stream isotopes are similarly affected by soil and stream parameters, and show significant influence of the newly introduced

45 snowmelt fractionation parameters (slope and amplification parameters). As anticipated, soil moisture simulations are most
46 sensitive to soil parameters, with the most sensitivity related to the porosity. The parameter sensitivity of frost depth was also
47 tested due to the newly implemented frost module. The frost depth was most sensitive to the snow temperature damping
48 parameter, with other sensitivity related to winter and thermal processes (snowmelt coefficient and soil thermal conductivity).
49 Since it is not possible to directly calibrate the soil water or streamflow water ages, the sensitivity analysis was evaluated to
50 provide additional assessment of which parameterizations will result in changes and uncertainties of the water ages. Except for
51 the soil heat capacity (set to $2.205 \times 10^6 \text{ W kg}^{-1} \text{ C}^{-1}$), residual soil moisture (set to 0.05), and the temperature at the damping depth
52 (set to 5°C), all other soil parameters (Fig B.1) were used in calibration since they showed to be sensitive for the calibration time-
53 series. Vegetation parameters used in calibration included the canopy water storage, leaf area index, maximum stomatal
54 conductance ($G_{s,\text{max}}$) and two soil-based vegetation parameters controlling the sensitivity of vegetation to suction potential and
55 moisture content.

56 ***Appendix C: Model calibration parameters***

57 Model calibration showed a reduction in the parameter space for almost all parameters, where the maximum range of parameters
58 is shown with the upper and lower bounds of the plots (Fig C.1). Differences between parameterization of soils was most
59 noticeable for anisotropy, hydraulic conductivity (K_h) and porosity (ϕ), while for vegetation, canopy storage, maximum stomatal
60 conductance ($G_{s,\text{max}}$) and leaf area index (LAI) varied most between the vegetation types.

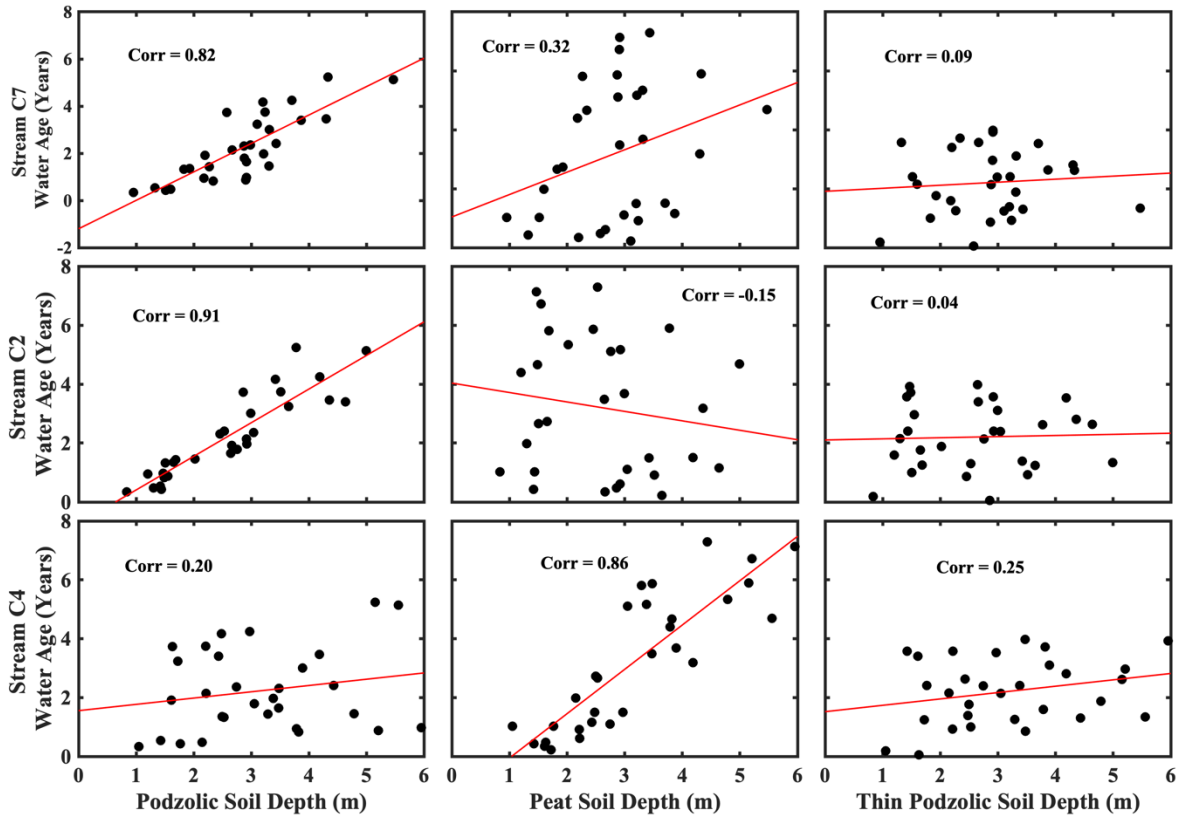


61

62 **Figure C.1: Calibration parameterization for soil and vegetation parameters for each soil and vegetation type. Lines represent the 25-**
 63 **75th quantiles and circles are outliers for the quartiles.**

64 ***Appendix D: Simulated layer depth vs. stream water ages***

65 Stream water ages were expected to be predominantly controlled by the depth of the third soil layer in each of the soil types (Fig
 66 B.1). The relatively old stream water ages observed within the simulations were on the upper end of the previously simulated
 67 water ages, with median ages of ~3 years for all streams. A direct correlation was observed for each stream to the depth of the
 68 dominant soil type of the sub-catchment. The overall catchment outlet (C7) was dominated by podzolic soils, and showed a
 69 strong (0.82 correlation coefficient) 1:1 relationship with a regression of the stream water age to the depth of the soil water (1
 70 year of stream age for each meter of soil depth) (Fig D.1). A similar, stronger, 1:1 relationship of stream water age to soil depth
 71 was observed at the outlet of sub-catchment C2, which was also dominated by podzolic soils (Fig D.1). Unsurprisingly, in the
 72 peat dominated C4 catchment, a strong relationship (0.86 correlation coefficient) was observed between the peat soil depth and
 73 stream water age; however, the stream water became older with soil depth than in the podzolic soil dominated catchments.



74

75

Figure D.1: Linear regression and correlation coefficients for stream water age at each sub-catchment against the soil depth